Critical Density-Wave Vestigial Phases of Commensurate Pair Density Wave

Chu-Tian Gao[1], Jing Zhou[2*], Yu-Bo Liu[3], and Fan Yang[1*]

[1]*School of Physics, Beijing Institute of Technology, Beijing 100081, China*
[2]*School of Electronic Science and Engineering, Chongqing University of Posts and Telecommunications, Chongqing 400065, China*
[3]*Institute of Theoretical Physics, Chinese Academy of Sciences, Beijing 100190, China*

(Received 7 December 2025; accepted manuscript online 24 March 2026)

The pair density wave (PDW) is an exotic pairing state hosting a spatially modulated pairing order parameter, which has attracted great interest. Due to its simultaneously breaking $U(1)$-gauge and translational symmetries, intriguing vestigial phases which restore only one broken symmetry can emerge at an intermediate temperature regime. Previously, investigations on the vestigial phases of PDW were mainly focused on incommensurate PDW. However, the experimentally observed PDW is usually commensurate, whose vestigial phases have not been systematically investigated. Here we study the vestigial phases of 2D commensurate PDW with n-times ($n \geq 3$) expanded unit vectors, hosting different numbers of wave vectors. Based on the Ginzburg–Landau theory, we get the low energy effective model Hamiltonian from typical PDW ground state configurations. Subsequent renormalization group (RG) and Monte-Carlo (MC) studies are conducted to obtain the phase diagram and spatial dependent correlation functions. Our RG and MC calculations consistently yield the following result. For $nt \leq 4$ ($t = 1$ for odd n and $t = 1/2$ for even n), besides the charge-$4e/2e$ superconductivity, there exists the translational symmetry broken charge-density-wave (CDW) vetigial phase. Intriguingly, for $nt \geq 5$ (specifically, for odd n, $n \geq 5$, and for even n, $n \geq 10$), the restoration of the translational symmetry with increasing temperature is realized through two successive Berezinskii–Kosterlitz–Thouless transitions. Such a two-step process leads to two critical vestigial phases, i.e., the critical-PDW and the critical-CDW phases, in which the discrete translational symmetry is quasily broken, leading to a power-law decaying density–density correlation even at 2D. Our work appeals for experimental verifications.

DOI: 10.1088/0256-307X/43/5/050704 CSTR: 32039.14.0256-307X.43.5.050704

Introduction. The pair density wave (PDW) is an unconventional superconducting state in which Cooper pairs carry a non-zero center-of-mass momentum, characterized by a spatially modulated pairing order.[1–19] Since the PDW is irrelevant in the weak-coupling renormalization group (RG) analysis,[20] its emergence suggests strong correlations. It has been identified in various correlated electron materials, exampled by Cuprate superconductors,[21–25] kagome lattice superconductors,[26,27] transition-metal dichalcogenide,[28] Iron-based superconducting materials,[29,30] Uranium-based heavy-fermion superconducting compounds[31] and may also exist in cold atomic systems.[32,33] These studies hold significant importance for understanding superconductivity (SC) in correlated electron systems.

The PDW state exhibits spontaneous breaking both translational and $U(1)$-gauge symmetry. As these two symmetries are generally not restored simultaneously, widespread interest has been ignited in characterizing the resultant vestigial phases.[4,34–54] For 2D incommensurate PDW, the ground state symmetry breaking is $U(1) \times U(1)$[34] or $U(1) \times U(1) \times U(1)$,[4,35] leading to two or three independent low-energy fluctuating phase modes. These low-energy phase modes can be rearranged into the total phase and the relative phase(s). When the relative phase(s) is (are) locked and the total phase is disordered, it implies that the $U(1)$ symmetry is restored while the translation symmetry is broken, leading to the charge density wave (CDW) phase. In contrast, when the total phase is locked and the relative phase(s) is (are) disordered, the translation symmetry is restored, whereas the $U(1)$ symmetry is broken. This results in the emergence of charge-$2e/4e/6e$ SC. The higher charge superconductivity with fractional flux quantization has been reported.[55–58]

While in real materials, the incommensurate PDW can be viewed as an approximation as a commensurate one with long period, most of the presently identified PDW states are commensurate ones with short period. For example, in copper-based materials, the PDW period is $4a_0$[21] and $8a_0$,[23,25] while in CsV_3Sb_5, the PDW period is $2a_0 \times 2a_0$.[26,27,59] The vestigial phases of commensurate PDW have not been systematically investigated yet, which will be the focus of our work. In particular, we shall address the following questions. What is the phase diagram for commensurate PDW? Are these phase diagrams dependent on the period of the PDW? Are there any exotic

*Corresponding authors. Email: zhoujing@cqupt.edu.cn; yangfan_blg@bit.edu.cn
© 2026 Chinese Physical Society and IOP Publishing Ltd. All rights, including for text and data mining, AI training, and similar technologies, are reserved.

phases in the phase diagrams which are unconventional for 2D electronic system?

In this paper, we explore the vestigial phases of commensurate PDW with periodicity $na_0 \times na_0$ ($n \geq 3$). Based on the Ginzburg–Landau (GL) theory, we derive the low-energy effective Hamiltonian which describes the pairing phase fluctuations of the commensurate PDW state with typical configurations. In particular, the relative phase fluctuates between its nt saddle points ($t = 1$ for odd n and $t = 1/2$ for even n), which is described by a nt-state clock model.[60–68] We determine the phase diagrams and phase transitions by combined RG and Monte–Carlo (MC) studies, which consistently yield the following results. For $nt \leq 4$, the previously known charge-$2e$/$4e$/$6e$ SC or long-range CDW state can be the intermediate vestigial phase between the low-temperature PDW ground state and the high-temperature normal metal (MT) state. For $nt \geq 5$ (i.e., for $n \geq 5$ if odd, or $n \geq 10$ if even), two additional critical vestigial phases emerge, i.e., the critical-PDW (C-PDW) and the critical-CDW (C-CDW), characterized by power-law decaying CDW correlation. Remarkably, the discrete translational symmetry is quasily broken even in 2D in these intriguing critical phases. Moreover, due to the presence of these critical phases, all the phase transitions in the phase diagram are Berezinskii–Kosterlitz–Thouless (BKT) transitions. This nt-dependent result is related to the properties of the nt-state clock model. Our results are highly anticipated for experimental verifications.

Model. Consider the PDW order parameter in a D_6- (or D_4-) symmetric system, characterized by multiple symmetry-related degenerate wave vectors $\{\boldsymbol{Q}_\alpha\}$:

$$\Delta(\boldsymbol{r}) = \sum_\alpha (\Delta_{\boldsymbol{Q}_\alpha} e^{i\boldsymbol{Q}_\alpha\cdot\boldsymbol{r}} + \Delta_{-\boldsymbol{Q}_\alpha} e^{-i\boldsymbol{Q}_\alpha\cdot\boldsymbol{r}}). \tag{1}$$

As shown in Fig. 1, the hexagonal $3Q$ PDW hosts three pairs of wave vectors $\pm\boldsymbol{Q_1}, \pm\boldsymbol{Q_2}, \pm\boldsymbol{Q_3}$ satisfying $\boldsymbol{Q}_1+\boldsymbol{Q}_2+\boldsymbol{Q}_3 = 0$, and the $2Q$ PDW hosts two pairs of wave vectors $\pm\boldsymbol{Q_1}, \pm\boldsymbol{Q_2}$. Let us focus on two typical ground states $\{\Delta_{\boldsymbol{Q}_1}, \Delta_{\boldsymbol{Q}_2}, \Delta_{\boldsymbol{Q}_3}, \Delta_{-\boldsymbol{Q}_1}, \Delta_{-\boldsymbol{Q}_2}, \Delta_{-\boldsymbol{Q}_3}\} = \Delta_0 e^{i\theta}\{e^{i\phi_1}, e^{i\phi_2}, e^{i\phi_3}, e^{-i\phi_1}, e^{-i\phi_2}, e^{-i\phi_3}\} \equiv \Delta_0\{e^{i\theta_1}, e^{i\theta_2}, e^{i\theta_3}, e^{i\theta_1'}, e^{i\theta_2'}, e^{i\theta_3'}\}$[35] and $\{\Delta_{\boldsymbol{Q}_1}, \Delta_{\boldsymbol{Q}_2}, \Delta_{-\boldsymbol{Q}_1}, \Delta_{-\boldsymbol{Q}_2}\} = \Delta_0 e^{i\theta}\{e^{i\phi_1}, e^{i\phi_2}, e^{-i\phi_1}, e^{-i\phi_2}\} \equiv \Delta_0\{e^{i\theta_1}, e^{i\theta_2}, e^{i\theta_1'}, e^{i\theta_2'}\}$ ($\Delta_0 > 0$)[4] for the two PDW states, respectively. Here θ and ϕ_α are free parameters, and we have $\theta_\alpha = \theta + \phi_\alpha$ and $\theta'_\alpha = \theta - \phi_\alpha$. Note that in the $3Q$ PDW state, the relative phases additionally satisfy $\phi_1 + \phi_2 + \phi_3 = 0$.[35]

At finite temperature, the thermal fluctuations lead to low-energy phase fluctuations of the PDW order parameter, so that these free parameters become phase fields: $\Delta_{\boldsymbol{Q}_\alpha} = \Delta_0 e^{i\theta_\alpha(\boldsymbol{r})}$, $\Delta_{-\boldsymbol{Q}_\alpha} = \Delta_0 e^{i\theta'_\alpha(\boldsymbol{r})}$, with $\theta_\alpha(\boldsymbol{r}) = \theta(\boldsymbol{r}) + \phi_\alpha(\boldsymbol{r})$ and $\theta'_\alpha(\boldsymbol{r}) = \theta(\boldsymbol{r}) - \phi_\alpha(\boldsymbol{r})$. The physical $\theta_\alpha(\boldsymbol{r})$ and $\theta'_\alpha(\boldsymbol{r})$ phase fields should host only integer vortices to ensure the single-valuedness of the superconducting order parameters. This restricts the allowed vortices in the θ and ϕ_α fields for different PDW states. For the $3Q$ PDW groundstate, only integer vortex and dislocation charge are allowed because $\phi_1+\phi_2+\phi_3 = 0$.[35] For the $2Q$ PDW case, since ϕ_1 and ϕ_2 are independent, θ and $\phi_{1,2}$ can simultaneously host integer or half-integer vortices,[4] respectively. This is the "kinematics constraint" between the θ and ϕ_α fields.[67,68]

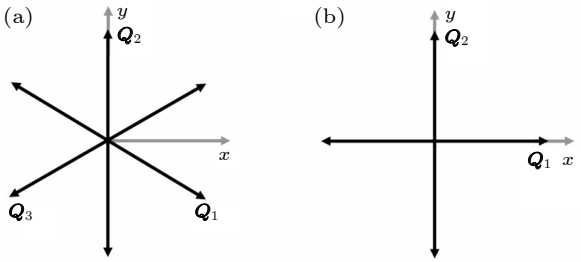

Fig. 1. Directions of $\boldsymbol{Q}_\alpha$, for (a) $3Q$ PDW and (b) $2Q$ PDW.

Let us derive the low-energy effective Hamiltonian for the phase fluctuations. Firstly, the spatial variation of the phase fields θ and ϕ_α costs the following energy H_0 which depends on the gradient of the fields,

$$H_0 = \int d^2\boldsymbol{r}\Big(\frac{\rho}{2}|\nabla\theta|^2 + \frac{\mu}{2}\sum_\alpha |\nabla\phi_\alpha|^2\Big). \tag{2}$$

Here ρ and μ are stiffness parameters for the total and relative phases, respectively. For the incommensurate PDW, Eq. (2) is already the full Hamiltonian.[4,35] However, for the commensurate PDW, there can be the following additional anisotropic term in the Hamiltonian. For a 2D commensurate PDW with the periodicity $na_0 \times na_0$ ($n \geq 3$), the wave vector $\boldsymbol{Q}_\alpha$ can be $\boldsymbol{Q}_\alpha = \frac{m_{1\alpha}}{n}\boldsymbol{b}_1 + \frac{m_{2\alpha}}{n}\boldsymbol{b}_2$, where $\boldsymbol{b}_{1,2}$ are the reciprocal lattice vectors, $m_{i\alpha}$ ($i = 1, 2$) and n are coprime integers. The Wigner–Seitz vectors are $\boldsymbol{a_1} = (a, 0)$ and $\boldsymbol{a_2} = (\frac{a}{2}, \frac{\sqrt{3}}{2}a)$ for $3Q$ PDW, $\boldsymbol{a}_1 = (a, 0)$, and $\boldsymbol{a}_2 = (0, a)$ for $2Q$ PDW. Under the translation $\boldsymbol{a}_i$, we have

$$\Delta_{\pm\boldsymbol{Q}_\alpha}(\boldsymbol{r}) \to \Delta_{\pm\boldsymbol{Q}_\alpha}(\boldsymbol{r} - \boldsymbol{a}_i)e^{\mp i\boldsymbol{Q}_\alpha\cdot\boldsymbol{a}_i}, \tag{3}$$

where $\boldsymbol{Q}_\alpha \cdot \boldsymbol{a}_i = 2\pi\frac{m_{i\alpha}}{n}$. The invariance of the free energy under this translation and the $U(1)$-gauge operation allows for the following anisotropic term:

$$\begin{aligned} F_{\rm ani} &= A_0\sum_\alpha (\Delta^{nt*}_{\boldsymbol{Q}_\alpha}(\boldsymbol{r})\Delta^{nt}_{-\boldsymbol{Q}_\alpha}(\boldsymbol{r}) + \text{c.c.}) \\ &= A\sum_\alpha \cos(2nt\phi_\alpha). \end{aligned} \tag{4}$$

Here A is proportional to $|\Delta_0|^{2nt}$, $t = 1$ for odd n and $t = 1/2$ for even n. There are other symmetry-allowed terms, but we assume that the coefficients of these terms are significantly smaller. Finally, the total low-energy effective Hamiltonian is

$$H = H_0 + A\int d^2\boldsymbol{r}\sum_\alpha \cos(2nt\phi_\alpha). \tag{5}$$

Equation (5) shows that while the θ field follows a conventional XY model that experiences a BKT transition when T increases, the ϕ_α field behaves like a XY model with q-fold ($q = nt$) anisotropy, resembling the symmetry of the q-state clock model. Note that θ_α and θ'_α are physical phase-angle variables that can be arbitrarily changed by 2π without altering the physical state, and so does $\Delta\theta_\alpha \equiv (\theta_\alpha - \theta'_\alpha)$. Then the definition $\phi_\alpha = \Delta\theta_\alpha/2$

suggests that there can be a π uncertainty in this definition of ϕ_α.[67,68] Consequently, while Eq. (5) appears $2nt$ saddle points for each ϕ_α field, these actually correspond to just nt physically distinct states, resulting in nt-fold anisotropy.

RG Study. We use the RG to study the Hamiltonian Eq. (5). In particular, for the 2D PDW state, only two of the ϕ_α fields are independent. We introduce two phonon fields $\boldsymbol{u} = (u_x, u_y)$[35] to simultaneously describe the $2Q$ and $3Q$ PDW states through the relation $\phi_\alpha = \boldsymbol{Q}_\alpha \cdot \boldsymbol{u}$, as for the $3Q$ state $\sum_\alpha \boldsymbol{Q}_\alpha = 0 \to \sum_\alpha \phi_\alpha = 0$. Then the Hamiltonian Eq. (5) can be rewritten as

$$H_{\text{eff}} = \int \mathrm{d}^2\boldsymbol{r}\Big[\frac{\rho}{2}|\nabla\theta|^2 + \frac{\mu}{2}\Big(\frac{2\pi}{a}\Big)^2|\nabla u_x|^2 + \frac{\mu}{2}\Big(\frac{2\pi}{a}\Big)^2|\nabla u_y|^2 + A\sum_\alpha \cos(2nt\phi_\alpha)\Big]. \quad (6)$$

As shown in Table 1, we have the vortex and dislocation charges of the topological excitations of the $3Q$ PDW and $2Q$ PDW phases by $\{\theta, u_x, u_y\}$. The corresponding action function of the multiple components Sine-Gordon model in dual space is

$$\begin{aligned} S_{\text{D}} = \int \mathrm{d}^2x_{\text{D}}\Big[&\frac{T}{2\rho}|\nabla\widetilde{\theta}|^2 + \frac{T}{2\mu}|\nabla\widetilde{u}_x|^2 + \frac{T}{2\mu}|\nabla\widetilde{u}_y|^2 \\ &+ g_\theta\cos 2\pi\widetilde{\theta} + g_x\cos\Big(\frac{2\pi a_{1x}\widetilde{u}_x}{a}\Big)\cos\Big(\frac{2\pi a_{1y}\widetilde{u}_y}{a}\Big) \\ &+ g_y\cos\Big(\frac{2\pi a_{2x}\widetilde{u}_x}{a}\Big)\cos\Big(\frac{2\pi a_{2y}\widetilde{u}_y}{a}\Big) + \sum_\alpha g_\alpha\cos(2nt\phi_\alpha) \\ &+ g^x_{\frac{1}{2}}\cos(\pi\widetilde{\theta})\cos(\pi\widetilde{u}_x) + g^y_{\frac{1}{2}}\cos(\pi\widetilde{\theta})\cos(\pi\widetilde{u}_y)\Big], \end{aligned} \quad (7)$$

where we have replaced $\frac{2\pi}{a}\widetilde{u}_i$ by $\widetilde{u}_i$ $(i = x, y)$. The dual bosonic field $\widetilde{\theta}$ and $\widetilde{u}_x, \widetilde{u}_y$ describe the vortice fields of θ and u_x, u_y. g_θ and g_x, g_y are proportional to the fugacities parameters of different integer vortex excitations. $g^x_{1/2}$, $g^y_{1/2}$ describe coupling parameters of half-half vortices. In the 3Q PDW state, only integer vortices are proliferated ($g^{x/y}_{1/2}$ does not exist).

In Table 2, we present fixed points of the tree level RG flow equations and corresponding phases in the vestigial phases of the commensurate PDW state. To simplify the expression, the half vortices coupling parameter $g^{x/y}_{1/2}$ is set as zero for $3Q$ PDW state. If g_θ or $g^{x/y}_{1/2}$ is relevant, suggesting the integer type votices or the half vortices are proliferated in the θ field, the superconductivity is killed. If $g_{x/y}$ or $g^{x/y}_{1/2}$ is relevant, suggesting the integer vortices or the half votices are proliferated in the $u_{x/y}$ field, the CDW is killed, and the translation symmetry is recovered. When $g_{x/y}$ and $g^{x/y}_{1/2}$ are irrelevant, if g_α are relevant, the translation symmetry is broken; while if g_α are irrelevant, the system enters critical phase. Since these coupling parameters are not simultaneously relevant and have the same sign, we do not consider frustration effects.[69]

The phase diagram for $2 \le nt \le 4$ is shown in Fig. 2(a). At low enough T, the fugacity parameter g_α is relevant while $g_\theta, g_{x/y}, g^{x/y}_{1/2}$ are all irrelevant, suggesting θ and $u_{x/y}$ are ordered and no vortices are proliferated, leading to the PDW phase. Enhancing T, when μ/ρ is small, translation symmetry is restored by proliferating integer vortices in dislocation while superconductivity still exists, leading to charge-$2e$ ($3Q$ PDW, described by order parameter $\Delta_{\boldsymbol{Q_1}}\Delta_{\boldsymbol{Q_2}}\Delta^*_{-\boldsymbol{Q_3}}$) or charge-$4e$ ($2Q$ PDW, characterized by the order parameter $\Delta_{\boldsymbol{Q_\alpha}}\Delta_{-\boldsymbol{Q_\alpha}}$) phase; when μ/ρ is large, g_θ becomes relevant by proliferating vortices in θ field while translation symmetry is still broken, leading to the CDW phase, which is described by $\Delta_{\boldsymbol{Q_\alpha}}\Delta^*_{-\boldsymbol{Q_\beta}}(\alpha \ne \beta)$ for the 3Q PDW and $\Delta_{\boldsymbol{Q_\alpha}}\Delta^*_{-\boldsymbol{Q_\alpha}}$ for the 2Q PDW. For large enough T, the fugacity parameters g_θ and $g_{x/y}$ (or $g^{x/y}_{1/2}$) become all relevant by proliferating vortices in θ and $u_{x/y}$ field, resulting in the normal MT phase. For intermediate regime of μ/ρ, there are two triple points for $2Q$ PDW case in the phase diagram, and the dashed line indicates a solid line which divides PDW phase and normal MT phase, suggesting the direct phase transition and all the orders are killed by half-half vortices proliferated ($g^{x/y}_{1/2}$ is relevant). For $3Q$ PDW case, only integer vortices are allowed to exist in θ or $u_{x/y}$ channel, so the dashed line decays into a quadruple point.

Table 1. The vortex and dislocation charges of the topological excitations of the $3Q$ PDW and $2Q$ PDW phases (n_α, $n_{\alpha'}$ and l_i are integers).

Phase	Vortex charge	Dislocation charge
$3Q$ PDW	$\frac{1}{2\pi}\oint \mathrm{d}\theta = n$	$\oint \mathrm{d}\boldsymbol{u} = l_1\boldsymbol{a_1}+l_2\boldsymbol{a_2}$
$2Q$ PDW	$\frac{1}{2\pi}\oint \mathrm{d}\theta = \frac{1}{2}(n_\alpha+n_{\alpha'})$	$\oint \mathrm{d}u_{x/y} = \frac{a}{2}(n_\alpha-n_{\alpha'})$

Table 2. Fixed points of the coupling parameters under RG, and the corresponding phases for the commensurate PDW. The abbreviations denote: $2e/4e$ SC is charge $2e$ SC and charge $4e$ SC; MT is normal metal; PDW is pair density wave; CDW is charge density wave; C-PDW is critical pair density wave; C-CDW is critical charge density wave.

g_θ	$g_{x/y}$	$g^{x/y}_{1/2}$	g_α	Phase
∞	∞	0	0	MT
∞	0	∞	0	MT
∞	0	0	∞	CDW
∞	0	0	0	C-CDW
0	0	0	∞	PDW
0	0	0	0	C-PDW
0	∞	0	0	Charge-$2e$/$4e$ SC

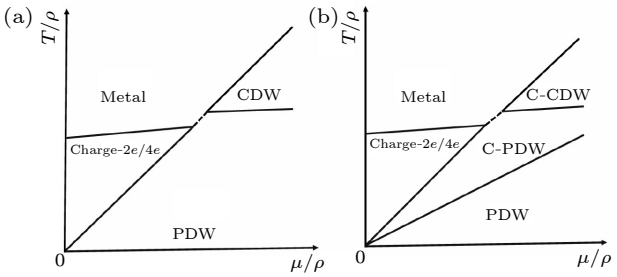

Fig. 2. Schematic phase diagrams of the commensurate PDW with (a) for $2 \le nt \le 4$ and (b) for $nt \ge 5$. ρ, μ, and T denote the superfluid stiffness, the CDW elastic constant and temperature, respectively. The black lines mark the phase boundaries. The dashed line represents a point for the 3Q PDW, while it represents for a solid line for the 2Q PDW.

Table 3. The correlation functions η_θ and η_{ϕ_α} decay for all possible phases in Fig. 2.

Phase	η_θ	η_{ϕ_α}
$2e/4e$ SC	$r^{-\sigma}$	$e^{-r/\xi}$
MT	e^{-r/ξ_1}	e^{-r/ξ_2}
PDW	$r^{-\sigma}$	Const
CDW	$e^{-r/\xi}$	Const
C-PDW	$r^{-\sigma_1}$	$r^{-\sigma_2}$
C-CDW	$e^{-r/\xi}$	$r^{-\sigma}$

The phase diagram for $nt \geq 5$ is shown in Fig. 2(b), wherein two new phases emerge: the C-PDW and the C-CDW. Their order parameters are the same as those of PDW and CDW, respectively. For these critical phases, $g_{x/y}$, $g_{1/2}^{x/y}$ and g_α are all irrelevant, suggesting that the translation symmetry is quasi broken. At low enough T, the system is PDW. When T increases, the systems will first enter the C-PDW phase in which all fugacity parameters are irrelevant and then enter different phases depending on the value of μ/ρ. If μ/ρ is small, increasing T further, $g_{x/y}$ becomes relevant, suggesting the charge-$2e/4e$ phase. If μ/ρ is large, increasing T further, the system will enter the C-CDW phase wherein integer vortices proliferate in the θ field. For high enough T, the system enters the normal MT phase. There are also two triple points connected by a dashed line. For $2Q$ PDW case, the dashed line indicates a solid line separating the C-PDW and the normal MT phase. For $3Q$ PDW case, the dashed line decays into a quadruple point.

The difference between the phase diagrams for $nt \leq 4$ and $nt \geq 5$ can be understood from the nt-state clock model[60] describing the $u_{x,y}$ fields. For this model, for $nt \leq 4$, the system will experience a second-order phase transition from the low-T ordered phase to high-T disordered phase; for $nt \geq 5$, the system will experience two subsequent BKT transitions first from the low-T ordered phase to the intermediate-T critical phase and then to the high-T disordered phase. The intermediate-T critical phase for $nt \geq 5$ just corresponds to the C-PDW and the C-CDW phases obtained here.

MC Study. To perform the MC study, we discretize the continuous Hamiltonian (5) on the square lattice as

$$\begin{aligned} H = & -\kappa \sum_{\langle ij \rangle} \cos[m\theta(\boldsymbol{r}_i) - m\theta(\boldsymbol{r}_j)] \\ & -\lambda \sum_{\langle ij \rangle,\alpha} \cos[m\phi_\alpha(\boldsymbol{r}_i) - m\phi_\alpha(\boldsymbol{r}_j)] \\ & -\gamma \sum_{\langle ij \rangle,\alpha} \{\cos[\theta(\boldsymbol{r}_i) + \phi_\alpha(\boldsymbol{r}_i) - \theta(\boldsymbol{r}_j) - \phi_\alpha(\boldsymbol{r}_j)] \\ & + \cos[\theta(\boldsymbol{r}_i) - \phi_\alpha(\boldsymbol{r}_i) - \theta(\boldsymbol{r}_j) + \phi_\alpha(\boldsymbol{r}_j)]\} \\ & + A \sum_{i,\alpha} \cos[2nt\phi_\alpha(\boldsymbol{r}_i)]. \end{aligned} \tag{8}$$

Here $\langle ij \rangle$ represents nearest-neighbor bonding and the coefficients κ, λ, and γ satisfy

$$\kappa = \frac{\rho - 4\gamma}{m^2}, \quad \lambda = \frac{\mu - 2\gamma}{m^2}, \tag{9}$$

with $m = 1, \gamma = 0$ for the $3Q$ PDW, and $m = 2, \gamma > 0$ for the $2Q$ PDW. The positive coefficients κ, λ, and γ ensure the discretized Hamiltonian (8) matches the continuous Hamiltonian (5) in the thermodynamic limit, respectively. Note that we have set $m = 2$ and finite $\gamma > 0$ for the case of $2Q$ PDW due to the following reason. Firstly, $m = 2$ energetically allows for integer and half-integer vortices of the θ and ϕ_α fields, as required by Table 1. Secondly, the γ term with $\gamma > 0$ energetically only allows for integer θ_α and θ_α' vortices, imposing the kinematic constraint between the θ and ϕ_α fields: they can either both host integer vortices or both host half-integer vortices, as implied by Table 1. This ensures the correct topology of the phase diagram for the $2Q$ PDW.[67,68] In the following MC studies, we set $\gamma = \frac{1}{4}\rho\mu/(\rho + \mu)$.

The nature of all phases can be characterized by the correlation function $\eta_{\theta/\phi_\alpha}$ for the θ and ϕ_α fields. The dependence of these functions on Δr ($\equiv |\Delta \boldsymbol{r}|$) for each phase is summarized in Table 3. See their formulas in the Supplementary Material (SM). An exponential decay in η_θ, signaling $U(1)$ gauge symmetry restoration, destroys superconductivity. In contrast, an exponential decay in η_{ϕ_α} restores translational symmetry and leads to a spatially uniform state, distinct from a density wave. When η_{ϕ_α} exhibits power-law decay, and η_θ exhibits either power-law or exponential decay, they correspond to C-PDW or C-CDW, respectively. The phase diagrams for different n from our MC simulations qualitatively agree with the RG results, as schematically illustrated in Fig. 2.

For $nt \leq 4$, as depicted in Fig. 2(a), when the temperature is low enough, η_θ follows a power law decay with Δr, and η_{ϕ_α} saturates to a finite value as $\Delta r \to \infty$, reflecting the PDW. If μ/ρ is small, increasing the temperature, while η_θ exhibits a power-law decay with Δr, η_{ϕ_α} shows exponential decay with Δr, reflecting the charge-$2e/4e$ SC; if μ/ρ is large, raising the temperature, whereas η_θ decays exponentially with Δr, η_{ϕ_α} saturates to a finite value as $\Delta r \to \infty$, reflecting the CDW. When the temperature is high enough, both η_θ and η_{ϕ_α} decay exponentially with Δr, reflecting the MT. When μ/ρ is moderate, a dashed line appears in the phase diagram. However, its physical meaning differs: it marks a solid-phase boundary for the $2Q$ PDW, whereas it physically degenerates to a single point for the $3Q$ PDW.

For $nt \geq 5$, as depicted in Fig. 2(b), in addition to the phases mentioned above, there are two other phases that require particular emphasis in our study. We provide the correlation functions in Fig. 3 for the two critical phases of the $3Q$ PDW. The correlation functions in the two critical phases of the 2Q PDW follow the same patterns. As the temperature increases, both η_θ and η_{ϕ_α} exhibit power-law decay with Δr [Figs. 3(a) and 3(c)]. The system transitions from the PDW state to the C-PDW state. As the temperature is further increased, the system enters a charge $2e/4e$ SC phase for small μ/ρ, a MT phase for intermediate μ/ρ, and a C-CDW phase for large μ/ρ. For the C-CDW phase, η_θ shows exponential decay with Δr and η_{ϕ_α} exhibits a power-law decay with Δr [Figs. 3(b) and 3(d)].

Notably, we have discovered two novel critical phases, C-PDW and C-CDW, which emerge only for the commensurate PDW with periodicity $nt \geq 5$ and are absent for

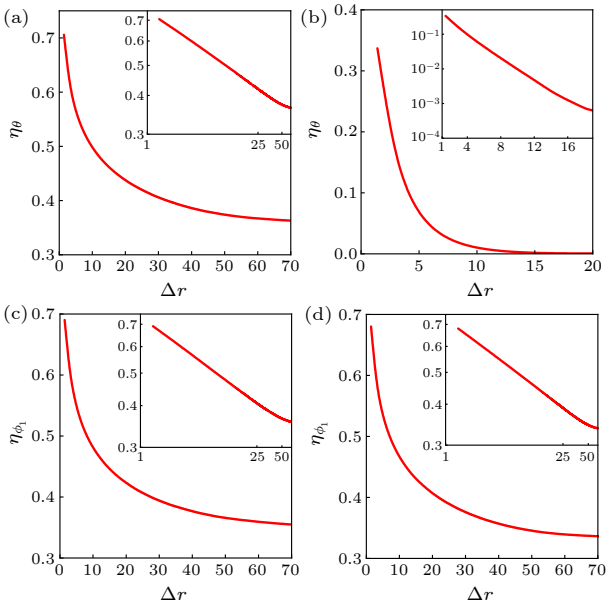

Fig. 3. The correlation functions η_{θ/ϕ_1} for the $3Q$ PDW are shown for the C-PDW phase in panels (a) and (c), and for the C-CDW phase in panels (b) and (d). Insets of [(a), (c), and (d)] the log-log plot, and (b) only the y-axis is logarithmic. Further details are provided in the SM.

$nt \leq 4$. In these phases, the correlation $\eta_{\phi_\alpha}(\Delta r)$ exhibits quasi-long-range order (QLRO), which can be regarded as the remarkable "quasi-breaking" of translation symmetry. We provide the detailed results of the hexagonal $3Q$ PDW and the $2Q$ PDW in the SM.

To investigate the nature of the phase transitions, we present the thermodynamic quantities as functions of temperature for different lattice sizes L, with details provided in the SM. These quantities include the specific heat C_v, the susceptibilities of the θ and ϕ_α fields, the Binder cumulant $3U_\theta - 1$ and $3U_{\phi_\alpha} - 1$, the stiffness S of θ field, the Ising order parameter I_α of ϕ_α field. As shown in Fig. 2(a), for systems with $nt \leq 4$, we find that for small μ/ρ, the enhancement of T first leads to a second-order phase transition in the ϕ_α field, followed by a BKT transition in the θ field. Conversely, for large μ/ρ, a BKT transition first occurs in the θ field, after which the ϕ_α field undergoes a second-order phase transition. For systems with $nt \geq 5$, as illustrated in Fig. 2(b), when μ/ρ is small, three successive BKT transitions occur: the first two are driven by the ϕ_α field, and the third is driven by the θ field. When μ/ρ is large, the system similarly exhibits three successive BKT transitions: first, the ϕ_α field undergoes a BKT transition, then the θ field undergoes a BKT transition, and finally, the ϕ_α field undergoes a second BKT transition. To conclude, for $nt \leq 4$, the ϕ_α field always undergoes a single second-order phase transition from long-range order (LRO) to disorder, while for $nt \geq 5$, it experiences two successive BKT transitions: first from LRO to QLRO, and then from QLRO to disorder. This behavior is consistent with the nt-state clock model.

Conclusion and Discussion. We have also studied the $1Q$ PDW, i.e., the unidirectional PDW with wave vectors $\pm\boldsymbol{Q}$, which is described by two complex gap functions $\Delta_{\pm\boldsymbol{Q}}(\boldsymbol{r})$.[34] In the incommensurate case, previous study[34] has yielded the charge-$4e$ SC ($\Delta_{\boldsymbol{Q}}\Delta_{-\boldsymbol{Q}}$) and CDW ($\Delta_{\boldsymbol{Q}}\Delta^*_{-\boldsymbol{Q}}$) as vestigial phases. Here we studied the commensurate case with period na_0 ($n \geq 3$). In comparison with the incommensurate case, the free energy for the commensurate PDW acquires an additional term, $(\Delta^{nt*}_{+\boldsymbol{Q}}(\boldsymbol{r})\Delta^{nt}_{-\boldsymbol{Q}}(\boldsymbol{r}) + \text{c.c.})$, as detailed in the SM. Considering the anisotropy in the x and y directions, our analysis therefore employs the MC simulations rather than the RG method. We find that the main result is qualitatively the same as the of the $2Q$ PDW shown in Fig. 2. In particular, for $nt \geq 5$, the C-PDW and C-CDW phases also emerge.

In this work, we only consider phase fluctuations in low-energy scales and therefore neglect the Higgs mode arising from amplitude fluctuations.[70] We focus on the typical ground-state configurations from Refs. [35] and [4] for the $3Q$ and $2Q$ PDW states, although similar results may hold for other ground states as well. We have constructed a simplified GL theory for commensurate PDW systems, with anisotropic terms $\sum_\alpha(\Delta^{nt*}_{\boldsymbol{Q}_\alpha}(\boldsymbol{r})\Delta^{nt}_{-\boldsymbol{Q}_\alpha}(\boldsymbol{r}) + \text{c.c.})$. It is worth noting that up to $2n$-th order in the expansion, there exist other additional symmetry-allowed terms [e.g., $\sum_{\alpha\neq\beta}(\Delta^{n*}_{\boldsymbol{Q}_\alpha}(\boldsymbol{r})\Delta^{n}_{\boldsymbol{Q}_\beta}(\boldsymbol{r}) + \text{c.c.}) \sim \sum_{\alpha\neq\beta}\cos(n\phi_\alpha - n\phi_\beta)$], which directly couple different ϕ_α components. In a more general theoretical framework, these terms may introduce richer physical phenomena, such as modifying the free-energy landscape or affecting the vortex excitation spectrum. Constructing and analyzing the complete general form of the GL theory up to $2n$-th order is a nontrivial task and lies beyond the scope of the present study. We hope that future work can systematically investigate these couplings to achieve a more comprehensive understanding of the complex phase behavior in commensurate PDW systems.

In conclusion, we have conducted a systematic investigation on the vestigial phases of 2D commensurate PDW in the form of $3Q$, $2Q$, and $1Q$. We find that the resultant phase diagrams differ for different periods n of the PDW with expanded unit cell $na_0 \times na_0$. Note that we are discussing the case where $n \geq 3$; for $n = 2$, our derivation and analysis do not apply. For $2 \leq nt \leq 4$ (for odd n, $t = 1$ and even n, $t = 1/2$), the systems exhibit charge-$2e$/$4e$ SC and CDW vestigial phases, which are known previously. The new discovery here is that for $nt \geq 5$, the translational symmetry undergoes a two-step transition first from LRO to QLRO and then from QLRO to disorder through two successive BKT transitions, leading to the two intermediate-temperature critical phases, C-PDW and C-CDW, as secondary orders. Our findings provide insights into vestigial phases in commensurate PDW.

Acknowledgements. F. Y. was supported by the National Natural Science Foundation of China (Grant Nos. 12574141, 12234016, and 12074031). J. Zhou was supported by the Scientific Research Program from Science and Technology Bureau of Chongqing City (Grant No. CSTB2025NSCQ-GPX1303). Y.-B. L. was supported by the postdoctoral innovation talent support program (Grant No. A5B10039).

References

[1] Fulde L and Ferrell R A 1964 *Phys. Rev.* **135** A550
[2] Larkin A and Ovchinikov Y N 1965 *JETP* **20** 762
[3] Radzihovsky L and Vishwanath A 2009 *Phys. Rev. Lett.* **103** 010404
[4] Agterberg D F and Tsunetsugu H 2008 *Nat. Phys.* **4** 639
[5] Wang C, Gao C, Jian C M, and Zhai H 2010 *Phys. Rev. Lett.* **105** 160403
[6] Cho G Y, Bardarson J H, Lu Y M, and Moore J E 2012 *Phys. Rev. B* **86** 214514
[7] Lee P A 2014 *Phys. Rev. X* **4** 031017
[8] Maciejko J and Nandkishore R 2014 *Phys. Rev. B* **90** 035126
[9] Jian S K, Jiang Y F, and Yao H 2015 *Phys. Rev. Lett.* **114** 237001
[10] Jian S K, Lin C H, Maciejko J, and Yao H 2017 *Phys. Rev. Lett.* **118** 166802
[11] Jian S K, Scherer M M, and Yao H 2020 *Phys. Rev. Res.* **2** 013034
[12] Han Z, Kivelson S A, and Yao H 2020 *Phys. Rev. Lett.* **125** 167001
[13] Agterberg D F, Séamus Davis J C, Edkins S D *et al.* 2020 *Annu. Rev. Condens. Matter Phys.* **11** 231
[14] Berg E, Fradkin E, Kivelson S A, and Tranquada J M 2009 *New J. Phys.* **11** 115004
[15] Wang Y, Agterberg D F, and Chubukov A 2015 *Phys. Rev. Lett.* **114** 197001
[16] Wang Y, Agterberg D F, and Chubukov A 2015 *Phys. Rev. B* **91** 115103
[17] Jin J T, Jiang K, Yao H, and Zhou Y 2022 *Phys. Rev. Lett.* **129** 167001
[18] Yao M, Wang Y, Wang D, Yin J X, and Wang Q H 2025 *Phys. Rev. B* **111** 094505
[19] Yang F Z, Zhang H D, Mandal S, Meng F Y, Fabbris G, Said A H, Mercado Lozano P, Rajapitamahuni A, Vescovo E, Nelson C, Lin S, Park Y, Clements E M, Ward T Z, Lee H N, Lei H C, Liu C X, and Miao H 2025 *Nat. Commun.* **16** 6626
[20] Shankar R 1994 *Rev. Mod. Phys.* **66** 129
[21] Eisaki H, Uchida S, Lawler M J, Kim E A, Mackenzie A P, Fujita K, Lee J, and Davis J C S 2016 *Nature* **532** 343
[22] Ruan W, Li X, Hu C, Hao Z, Li H, Cai P, Zhou X, Lee D H, and Wang Y 2018 *Nat. Phys.* **14** 1178
[23] Du Z, Li H, Joo S H, Donoway E P, Lee J, Davis J C S, Gu G, Johnson P D, and Fujita K 2020 *Nature* **580** 65
[24] Li X, Zou C, Ding Y, Yan H, Ye S, Li H, Hao Z, Zhao L, Zhou X, and Wang Y 2021 *Phys. Rev. X* **11** 011007
[25] Edkins S D, Kostin A, Fujita K, Mackenzie A P, H. Eisaki H, Uchida S, Sachdev S, Lawler M J, Kim E A, Davis J C S, and Hamidian M H 2019 *Science* **364** 976
[26] Chen H, Yang H, Hu B, Zhao Z, Yuan J, Xing Y, Qian G, Huang Z, Li G, Ye Y, Ma S, Ni S, Zhang H, Yin Q, Gong C, Tu Z, Lei H, Tan H, Zhou S, Shen C, Dong X, Yan B, Wang Z, and Gao H J 2021 *Nature* **599** 222
[27] Han X, Chen H, Tan H, Cao Z, Huang Z, Ye Y, Zhao Z, Shen C, Yang H, Yan B, Wang Z, and Gao H J 2025 *Nat. Nanotechnol.* **20** 1017
[28] Liu X, Chong Y X, Sharma R, and Davis J C S 2021 *Science* **372** 1447
[29] Zhao H, Blackwell R, Thinel M, Handa T, Ishida S, Zhu X, Iyo A, Eisaki H, Pasupathy A N, and Fujita K 2023 *Nature* **618** 940
[30] Liu Y, Wei T, He G, Zhang Y, Wang Z, and Wang J 2023 *Nature* **618** 934
[31] Gu Q, Carroll J P, Wang S, Ran S, Broyles C, Siddiquee H, Butch N P, Saha S R, Paglione J, Davis J C S, and Liu X 2023 *Nature* **618** 921
[32] Liao Y a, Rittner A S C, Paprotta T, Li W, Partridge G B, Hulet R G, Baur S K, and Mueller E J 2010 *Nature* **467** 567
[33] Vitali E, Rosenberg P, and Zhang S 2022 *Phys. Rev. Lett.* **128** 203201
[34] Berg E, Fradkin E, and Kivelson S A 2009 *Nat. Phys.* **5** 830
[35] Agterberg D F, Geracie M, and Tsunetsugu H 2011 *Phys. Rev. B* **84** 014513
[36] You Y Z, Chen Z, Sun X Q, and Zhai H 2012 *Phys. Rev. Lett.* **109** 265302
[37] Babaev E 2004 *Nucl. Phys. B* **686** 397
[38] Ko W H, Lee P A, and Wen X G 2009 *Phys. Rev. B* **79** 214502
[39] Herland E V, Babaev E, and Sudbø A 2010 *Phys. Rev. B* **82** 134511
[40] Song F F and Zhang G M 2022 *Phys. Rev. Lett.* **128** 195301
[41] Li P, Jiang K, and Hu J 2024 *Sci. Bull.* **69** 2328
[42] Zhang L F, Wang Z, and Hu X 2024 *Commun. Phys.* **7** 210
[43] Zhou S and Wang Z 2022 *Nat. Commun.* **13** 7288
[44] Rampp M A, König E J, and Schmalian J 2022 *Phys. Rev. Lett.* **129** 077001
[45] Yu Y 2023 *Phys. Rev. B* **108** 054517
[46] Curtis J B, Poniatowski N R, Xie Y, Yacoby A, Demler E, and Narang P 2023 *Phys. Rev. Lett.* **130** 196001
[47] Poduval P P and Scheurer M S 2024 *Nat. Commun.* **15** 1713
[48] Zeng M, Hu L H, Hu H Y, You Y Z, and Wu C 2024 *Sci. China Phys. Mech. Astron.* **67** 237411
[49] Jian S K, Huang Y, and Yao H 2021 *Phys. Rev. Lett.* **127** 227001
[50] Fernandes R M and Fu L 2021 *Phys. Rev. Lett.* **127** 047001
[51] Hecker M, Willa R, Schmalian J, and Fernandes R M 2023 *Phys. Rev. B* **107** 224503
[52] Wu Y M and Wang Y 2024 *npj Quantum Mater.* **9** 66
[53] Song F F and Zhang G M 2022 *Phys. Rev. B* **105** 134516
[54] Varma C M and Wang Z 2023 *Phys. Rev. B* **108** 214516
[55] Ge J, Wang P, Xing Y, Yin Q, Wang A, Shen J, Lei H, Wang Z, and Wang J 2024 *Phys. Rev. X* **14** 021025
[56] Pan Z, Lu C, Yang F, and Wu C 2024 *Sci. China Phys. Mech. Astron.* **67** 287412
[57] Lin T Y, Song F F, and Zhang G M 2025 *Phys. Rev. B* **111** 054508
[58] Song F F and Zhang G M 2025 *Chin. Phys. Lett.* **42** 037401
[59] Deng H B, Qin H L, Liu G W *et al.* 2024 *Nature* **632** 775
[60] José J V, Kadanoff L P, Kirkpatrick S, and Nelson D R 1977 *Phys. Rev. B* **16** 1217
[61] Tobochnik J 1982 *Phys. Rev. B* **26** 6201
[62] Challa M S S and Landau D P 1986 *Phys. Rev. B* **33** 437
[63] Surungan T, Masuda S, Komura Y, and Okabe Y 2019 *J. Phys. A: Math. Theor.* **52** 275002
[64] Li Z Q, Yang L P, Xie Z Y, Tu H H, Liao H J, and Xiang T 2020 *Phys. Rev. E* **101** 060105
[65] Chen H, Hou P, Fang S, and Deng Y 2022 *Phys. Rev. E* **106** 024106
[66] Miyajima Y, Murata Y, Tanaka Y, and Mochizuki M 2021 *Phys. Rev. B* **104** 075114
[67] Liu Y B, Zhou J, Wu C, and Yang F 2023 *Nat. Commun.* **14** 7926
[68] Liu Y B, Zhou J, and Yang F 2024 *Phys. Rev. Lett.* **133** 136002
[69] Wu Y M, Murthy C, and Kivelson S A 2024 *Phys. Rev. Lett.* **133** 246501
[70] Wu Y M, Chubukov A V, Wang Y X, and Kivelson S A 2025 *npj Quantum Mater.* **10** 84